Supplement of Atmos. Chem. Phys., 25, 10267–10292, 2025
https://doi.org/10.5194/acp-25-10267-2025-supplement

Supplement of

Gas–particle partitioning of m-xylene and naphthalene oxidation products: temperature and NO_x influence

Marwa Shahin et al.

Correspondence to: Marwa Shahin (marwa.shahin@etu.univ-amu.fr) and Barbara D'Anna (barbara.danna@univ-amu.fr)

Supplementary method

Calculation of the carbon balance

The carbon balance was calculated by comparing the total carbon content of detected reaction products to the amount of carbon from the reacted precursor VOCs, with all quantities expressed in units of ppbC. First, the amount of precursor carbon reacted was determined by:

$$reacted\ carbon\ (ppbC)\ =\ \Delta[VOC]\ (ppb)\ \times\ n_C$$

where $\Delta[VOC]$ is the decrease in the VOC concentration due to its reaction, and n_C is the number of carbon atoms per molecule (8 for m-xylene, 10 for naphthalene).

Second, the carbon content of all observed products was calculated by summing the contribution of each compound:

$$product\ carbon\ (ppbC)\ =\ \sum_i ([product_i]\ (ppb)\ \times\ n_{C,i})$$

where $[product_i]$ is the measured mixing ratio and $n_{C,i}$ is the carbon number of each compound i.

The carbon balance was then computed as:

$$carbon\ balance\ (\%)\ =\ \frac{product\ carbon\ (ppbC)}{reacted\ carbon\ (ppbC)}\ \times\ 100$$

This calculation assumes that all carbon is either retained in the measured gas-phase or particle-phase products or converted into undetected species. It does not account for potential carbon in undetected products (e.g., oligomers, extremely low volatility species), or known small carbon products such as CO, CO_2, and glyoxal that we could not measure because of instrumental limitations.

Calculation of the OH rate constant

The values of the temperature dependent OH rate constant are calculated based on Arrhenius equation as follows:

$$k_{OH}\ (T) =\ A\ \frac{T}{298\ (K)}\ e^{\frac{-Ea}{RT}}$$

where

- k_{OH} (T) is the rate constant at temperature (T) [cm^3 $molecule^{-1}$ s^{-1}]
- T is the temperature [K]
- A is the pre-exponential factor
- R is the universal gas constant [8.413 J mol^{-1} K^{-1}]
- Ea is the activation energy [J mol^{-1}]

The specific parameters were (taken from NIST Kinetic Database):

- m-xylene: $A = 1.66 \times 10^{-11}$, Ea = -964 J mol^{-1}
- naphthalene: $A = 1.05 \times 10^{-12}$, Ea = -7500 J mol^{-1}

Calculation of the TSP

The SMPS measures number- and volume-based size distributions. In our analysis, we used the number concentration (particles cm^{-3}) measured by the SMPS and converted it to mass concentration (μg m^{-3}) by assuming spherical particles and applying the standard geometric volume formula for each size bin. Each calculated particle volume was then multiplied by the assumed composition-specific density to determine mass. Specifically, the densities used were: 1.0 g cm^{-3} for water, 1.4 g cm^{-3} for organics, and 1.7 g cm^{-3} for ammonium, sulfate and nitrate. The percentage of each chemical fraction for each experiment was inferred from AMS measurements, and the corresponding weighted average density was applied to the SMPS volume distribution to obtain TSP. This approach provided a more accurate representation of the aerosol mass.

Table S1. List of laboratory experiments conducted by Ng et al. (2007), Chen et al. (2018), Song et al. (2007), Chen et al. (2016) Chen et al. (2009), and their associated environmental conditions, such as chamber temperature, RH, VOC/NO$_x$ ratio, seeds mass and SOA yields.

	T	RH	VOC	NO$_x$	VOC/NO$_x$	Seeds	[OH]	ΔVOC	ΔM_0	Y
	K	%	ppbV	ppb	ppbC ppb^{-1}	µg m^{-3}	molecules cm^{-3}	µg m^{-3}	µg m^{-3}	%
Ng et al. (2007)	297	6	42-172 (not indicated for each exp)	943	high NO$_x$	AS	from HONO	71	18	5.9
	298	6		945	high NO$_x$	AS		28	4	3.5
	298	6		943	high NO$_x$	AS		133	46	8
	297	5		945	high NO$_x$	AS		106	37	8
Chen et al. (2018)	300	<0.1	44	8	high NO$_x$	none	3.04E+06	159	4.8	3
	300	<0.1	59	11.5	high NO$_x$	none	2.79E+06	201	11.6	6
Song et al. (2007)	300	<0.1	104	-	low NO$_x$	none	0.55E+06	193	17.3	8.9
	300	<0.1	112	-	low NO$_x$	none	0.84E+06	227	38	16.7
	300	<0.1	51	-	low NO$_x$	none	0.80E+06	113	20	17.7
	300	<0.1	39	-	low NO$_x$	none	1.05E+06	97	11.9	12.3
	300	<0.1	52	-	low NO$_x$	none	1.29E+06	147	45	30.6
	300	<0.1	46	-	low NO$_x$	none	1.18E+06	124	25	20.6
Chen et al. (2016)	RT	<0.1	45	698	high NO$_x$	none	from HONO	168	94.8	60
	RT	<0.1	29	776	high NO$_x$	none		126	59.4	47
	RT	<0.1	26	758	high NO$_x$	none		116	47.1	41
	RT	<0.1	30	776	high NO$_x$	none		105	3	3
	RT	<0.1	23	783	high NO$_x$	none		80	20.3	25
	RT	<0.1	28	22	low NO$_x$	none	from HONO	135	5.7	4
	RT	<0.1	15	13	low NO$_x$	none		76	21.1	28
	RT	<0.1	27	19	low NO$_x$	none		140	30.8	22
	RT	<0.1	35	10	low NO$_x$	none		173	50.1	29
	RT	<0.1	29	18	low NO$_x$	none		142	27.1	19
	RT	<0.1	17	11	low NO$_x$	none		84	26.2	31
	RT	<0.1	17	14	low NO$_x$	17.3		86	15.5	18
	RT	<0.1	16	21	low NO$_x$	41.9		77	9.7	13
	RT	<0.1	27	18	low NO$_x$	15.4		125	34.5	28
	RT	<0.1	15	10	low NO$_x$	3.4		69	22.7	33

Chan et al. (2009)	299	5-8	12	494	high NO_x	AS		59	10.9	19
	299	5-8	21	377	high NO_x	AS		93	27.7	30
	299	5-8	10	424	high NO_x	AS	from HONO	40	8	20
	299	5-8	17	477	high NO_x	AS		65	13.6	21
	299	5-8	17	477	high NO_x	AS		84	22.8	27

Table S2. Derived and estimated $\log_{10}C_i^*$ values for m-xylene products

Carbon number	Measured m/z and ion sum formula	Tentative assignment	SMILES string	Derived values			Estimated values		
				$\log_{10}C_i^*$ at 295 K	$\log_{10}C_i^*$ at 280 K	$\Delta\log_{10}C_i^*$	$\log_{10}C_i^*$ at 295 K	$\log_{10}C_i^*$ at 280 K	$\Delta\log_{10}C_i^*$
8	121.06 $(C_8H_8O).H^+$	tolualdehdye	CC1=CC(=CC=C1)C=O	3.72	3.66	0.06	6.03	5.65	0.38
8	171.07 $(C_8H_{10}O_4).H^+$	dimethyl-hexadienedioic acid dihydroxy-dimethyl-cyclohexene-dine	C/C(=C\C(=O)O)/C=C(\C)/C(=O)O CC1=CC(=O)C(C(C1=O)(C)O)O	1.12	0.83	0.30	0.87 0.78	0.30 0.21	0.58 0.58
8	153.06 $(C_8H_8O_3).H^+$	hydroxy-methylbenzoic acid	Cc1cccc(C(=O)O)c1O	2.19	2.07	0.12	1.78	1.29	0.49
8	187.06 $(C_8H_{10}O_5).H^+$	oxo-cyclohexane-dicarboxylic acid hydroxy-cyclohexene-dicarboxylic acid	C1C(CC(=O)CC1C(=O)O)C(=O)O C(C(=O)O)1C(C(O)=O)CC=CC1O	0.78	0.69	0.09	0.19 -1.19	-0.45 -1.95	0.64 0.76
7	141.05 $(C_7H_8O_3).H^+$	oxohepta-dienoic acid	CC(=O)/C=C/C=C/C(=O)O	1.74	1.41	0.33	3.86	3.33	0.53
7	154.05 $(C_7H_7NO_3).H^+$	nitrocresol	Cc1c(cccc1O)[N+](=O)[O-]	2.51	2.39	0.12	5.83	5.37	0.46
6	127.04 $(C_6H_6O_3).H^+$	dimethyl furandione	CC1=C(C)C(=O)OC1=O	1.95	1.79	0.17	5.46	5.06	0.40
6	129.06 $(C_6H_8O_3).H^+$	hydroxy-dioxohexanal methyl-oxo-pentenoic acid	CC(=O)C(O)CC(=O)C=O CC(=CC(=O)O)C(=O)C	1.73	1.31	0.43	3.58 4.36	3.07 3.87	0.52 0.49
5	113.02 $(C_5H_4O_3).H^+$	methylfuran-dione	CC1=CC(=O)OC1=O	3.45	3.11	0.34	5.85	5.46	0.39
5	131.04 $(C_5H_6O_4).H^+$	hydroxy-methyl-oxosuccinaldehyde	CC(C=O)(C(=O)C=O)O	2.54	2.13	0.40	3.55	3.11	0.43
5	115.03 $(C_5H_6O_3).H^+$	oxopentenoic acid	C=CC(=O)CC(=O)O	2.14	1.72	0.41	4.74	4.27	0.47
5	97.03 $(C_5H_4O_2).H^+$	furaldehyde (furfural)	C1=COC(=C1)C=O	2.56	2.27	0.30	6.52	6.18	0.34
5	117.05 $(C_5H_8O_3).H^+$	oxo-pentanoic acid	CC(=O)CCC(=O)O	2.62	2.00	0.62	4.85	4.39	0.46
5	101.06 $(C_5H_8O_2).H^+$	oxo-pentanal	CC(=O)CCC=O	1.99	1.40	0.59	6.99	6.64	0.35
4	71.05 $(C_4H_6O).H^+$	dihydrofuran MVK MAC	C1COC=C1 CC(=O)C=C CC(=C)C=O	2.90	2.26	0.65	8.75 8.51 8.10	8.51 8.24 7.83	0.24 0.27 0.26
4	103.04 $(C_4H_6O_3).H^+$	hydroxy oxobutanal	C(CO)C(=O)C=O	1.76	0.84	0.92	5.23	4.79	0.44
3	73.03 $(C_3H_4O_2).H^+$	methylglyoxal	CC(=O)C=O	3.16	2.69	0.47	7.72	7.45	0.27

3	75.04 $(C_3H_6O_2).H^+$	propanoic acid	CCC(=O)O	3.26	3.06	0.20	6.45	6.10	0.35

Table S3. Derived and estimated $\log_{10}C_i^*$ values for naphthalene products

Carbon number	Measured m/z and ion sum formula	Tentative assignment	SMILES string	Derived values			Estimated values		
				$\log_{10}C_i^*$ at 295 K	$\log_{10}C_i^*$ at 280 K	$\Delta\log_{10}C_i^*$	$\log_{10}C_i^*$ at 295 K	$\log_{10}C_i^*$ at 280 K	$\Delta\log_{10}C_i^*$
10	161.06 $(C_{10}H_8O_2).H^+$	formyl cinnamaldehyde	C1=CC=C(C(=C1)/C=C/C=O)C=O	1.91	1.20	0.71	3.85	3.25	0.60
10	193.05 $(C_{10}H_8O_4).H^+$	carboxy cinnamic acid	O=C(O)/C=C/c1ccccc1C(=O)O	1.28	1.15	0.13	-0.52	-1.17	0.65
10	159.04 $(C_{10}H_6O_2).H^+$	naphthoquinone	c1ccc2c(c1)C(=O)C=CC2=O	2.61	1.79	0.82	4.65	4.16	0.49
10	177.05 $(C_{10}H_8O_3).H^+$	formyl cinnamic acid	O=Cc1ccccc1/C=C/C(=O)O	1.44	1.24	0.20	1.66	1.07	0.60
10	175.04 $(C_{10}H_6O_3).H^+$	epoxy-naphthoquinone	C1=CC=CC2C(=O)C3OC3C(=O)C1=2	1.82	1.68	0.14	4.12	3.54	0.58
10	145.07 $(C_{10}H_8O).H^+$	naphthol	c1ccc2c(c1)cccc2O	1.75	1.21	0.54	3.78	3.28	0.50
10	191.04 $(C_{10}H_6O_4).H^+$	dihydroxy naphthoquinone	C1=C(O)C(O)=CC2C(=O)C=CC(=O)C1=2	1.81	1.66	0.15	0.49	-0.25	0.74
10	195.06 $(C_{10}H_{10}O_4).H^+$	phenylenediacetic acid carboxybenzenepropanoic acid	c1ccc(c(c1)CC(=O)O)CC(=O)O c1ccc(c(c1)CCC(=O)O)C(=O)O	1.79	1.50	0.29	-0.41 -0.42	-1.05 -1.04	0.64 0.63
10	174.05 $(C_{10}H_7NO_2).H^+$	nitronaphthalene	c1ccc2c(c1)cccc2[N+](=O)[O-]	3.07	2.32	0.75	3.85	3.37	0.48
10	190.05 $(C_{10}H_7NO_3).H^+$	nitronaphthol	c1ccc2c(c1)c(ccc2O)[N+](=O)[O-]	1.81	1.58	0.23	3.94	3.38	0.55
9	147.05 $(C_9H_6O_2).H^+$	benzopyrone (coumarin) indene-dione	c1ccc2c(c1)ccc(=O)o2 c1ccc2c(c1)C(=O)CC2=O	2.16	1.60	0.56	5.16 5.16	4.67 4.66	0.49 0.50
9	163.04 $(C_9H_6O_3).H^+$	hydroxycoumarin	c1ccc2c(c1)c(cc(=O)o2)O	1.90	1.75	0.15	3.08	2.50	0.58
9	133.06 $(C_9H_8O).H^+$	indanone	c1ccc2c(c1)CCC2=O	2.63	1.63	1.00	5.37	4.94	0.44
9	179.04 $(C_9H_6O_4).H^+$	dihydroxy-indene-dione	C1=CC=CC2C(=O)C(O)(O)C(=O)C1=2	1.63	0.54	1.08	3.05	2.35	0.69
9	165.06 $(C_9H_8O_3).H^+$	hydroxy cinnamic acid	c1ccc(c(c1)/C=C/C(=O)O)O	2.05	1.61	0.44	1.28	0.70	0.58
9	181.05 $(C_9H_8O_4).H^+$	dihydroxycinnamic acid	C1=CC(O)=CC(/C=C/C(=O)O)=C1O	1.64	1.41	0.23	-0.80	-1.51	0.70

8	135.05 ($C_8H_6O_2$).H^+	phthaldialdehyde	O=Cc1ccccc1C=O	3.32	2.16	1.06	4.73	4.27	0.46
8	149.03 ($C_8H_4O_3$).H^+	phthalic anhydride	c1ccc2c(c1)C(=O)OC2=O	3.16	2.76	0.39	5.10	4.62	0.49
8	151.04 ($C_8H_6O_3$).H^+	hydroxy phthalide	C1=CC=CC(C(=O)O)=C1C=O	2.11	1.50	0.61	2.57	2.02	0.55
		hydroxy phthalaldehyde	C1=CC(O)=CC(C=O)=C1C=O				2.65	2.11	0.54
6	115.07 ($C_6H_{10}O_2$).H^+	dimethyloxolanone	CC1CC(OC1=O)C	3.24	2.40	0.84	7.73	7.33	0.40
		hexanedione	CC(=O)CCC(=O)C				7.03	6.65	0.38

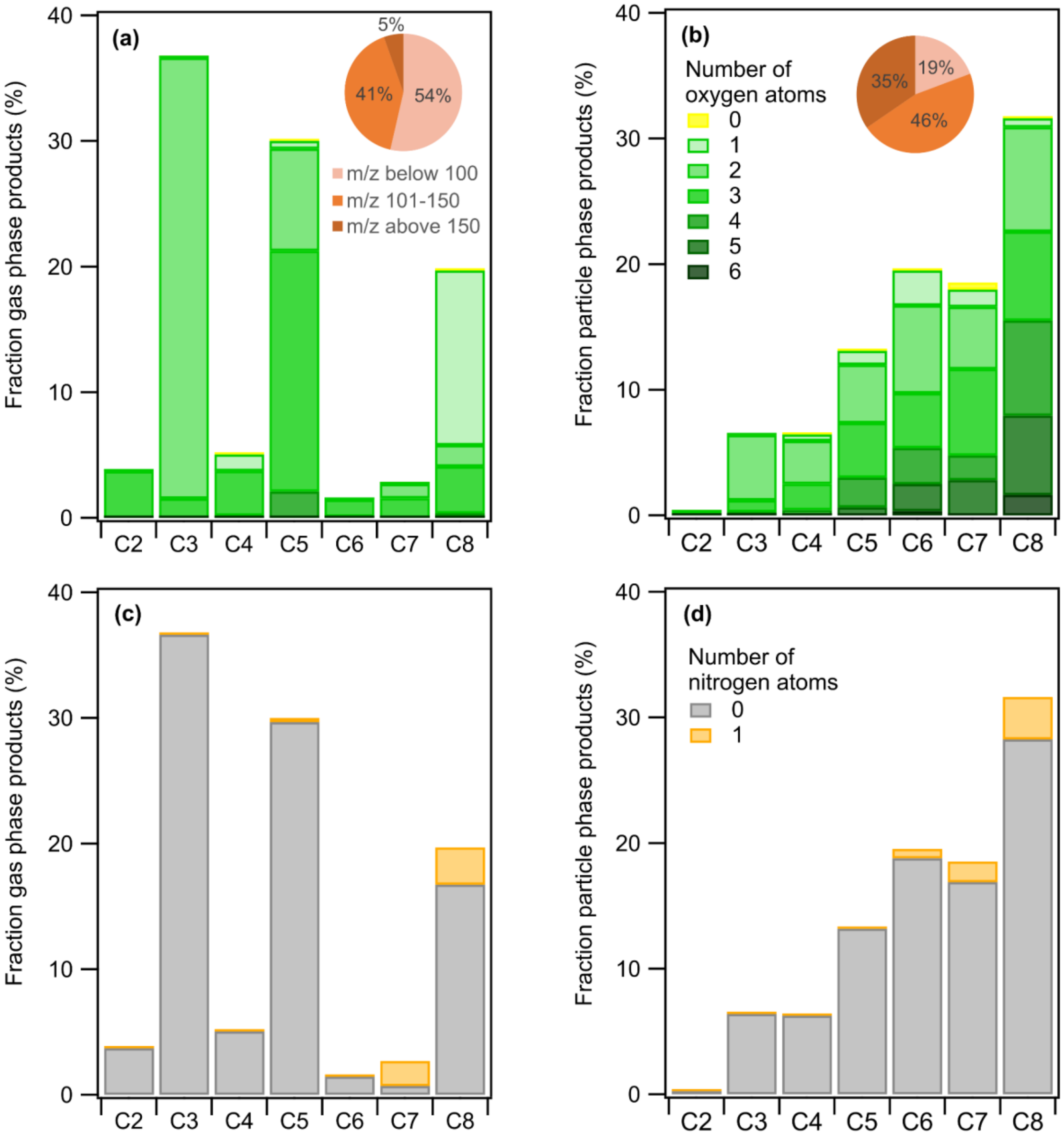

Figure S1. m-xylene mass products fraction (y-axis) distribution based on the number of carbon atoms (x-axis) for a high NO_x experiment 295 K, colored by the number of (a,b) oxygen and (c,d) nitrogen atoms. Detected compounds are in the (a,c) gas phase and (b,d) particle phase. Pie charts correspond to the molecular weight contribution to the overall mass.

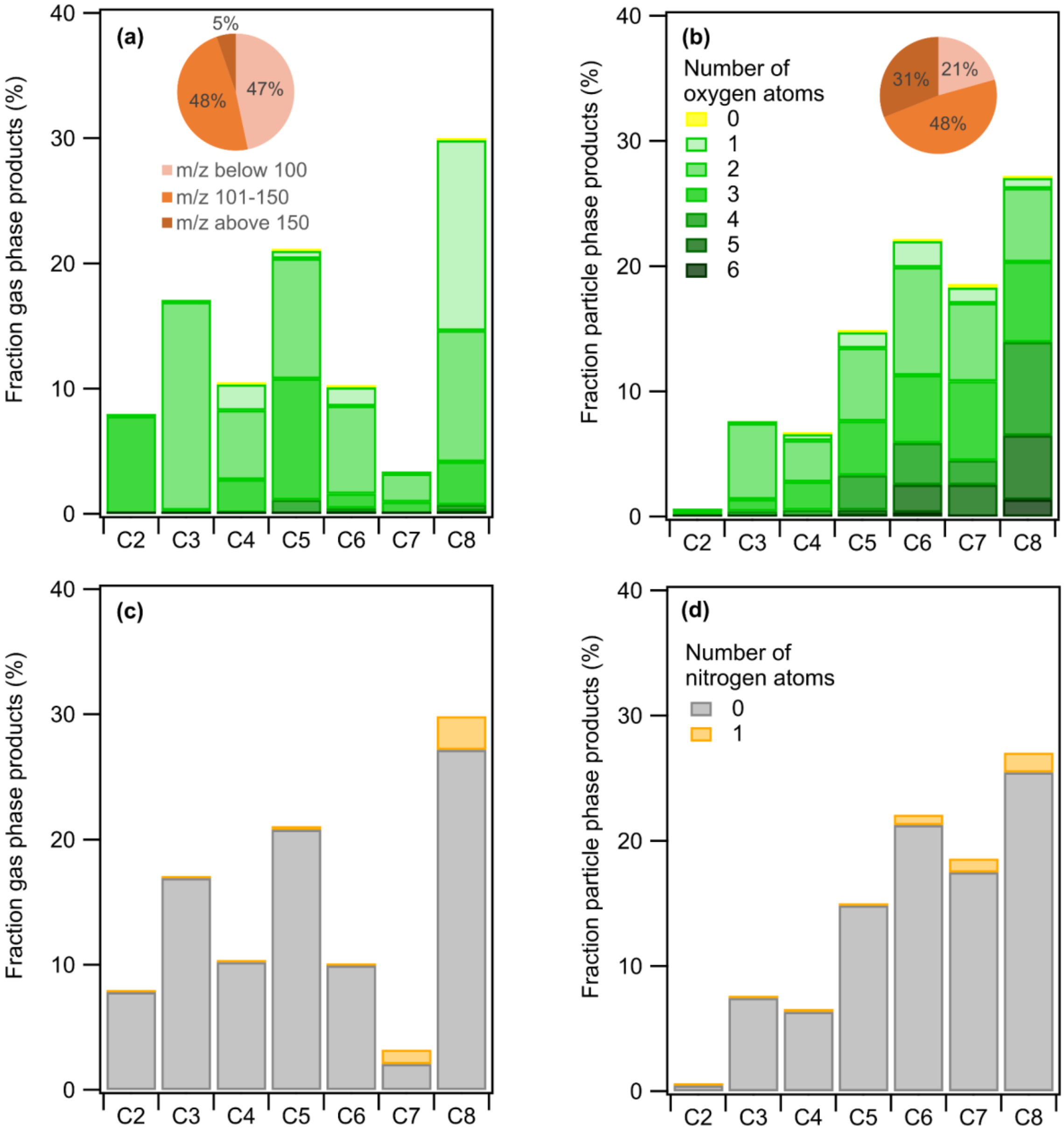

Figure S2. m-xylene mass products fraction (y-axis) distribution based on the number of carbon atoms (x-axis) for a low NO_x experiment 295 K, colored by the number of (a,b) oxygen and (c,d) nitrogen atoms. Detected compounds are in the (a,c) gas phase and (b,d) particle phase. Pie charts correspond to the molecular weight contribution to the overall mass.

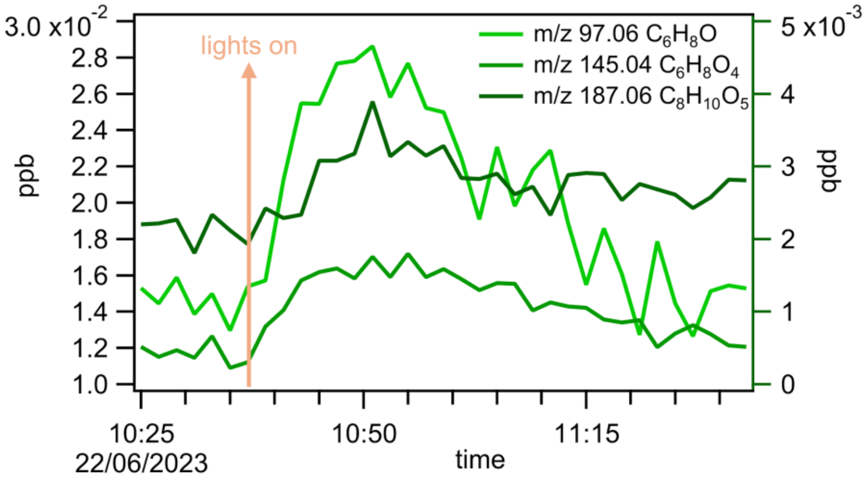

Figure S3. Time evolution of some C_6 and C_8 compounds in the gas phase at 295 K high NO_x experiment upon starting oxidation in the flow tube.

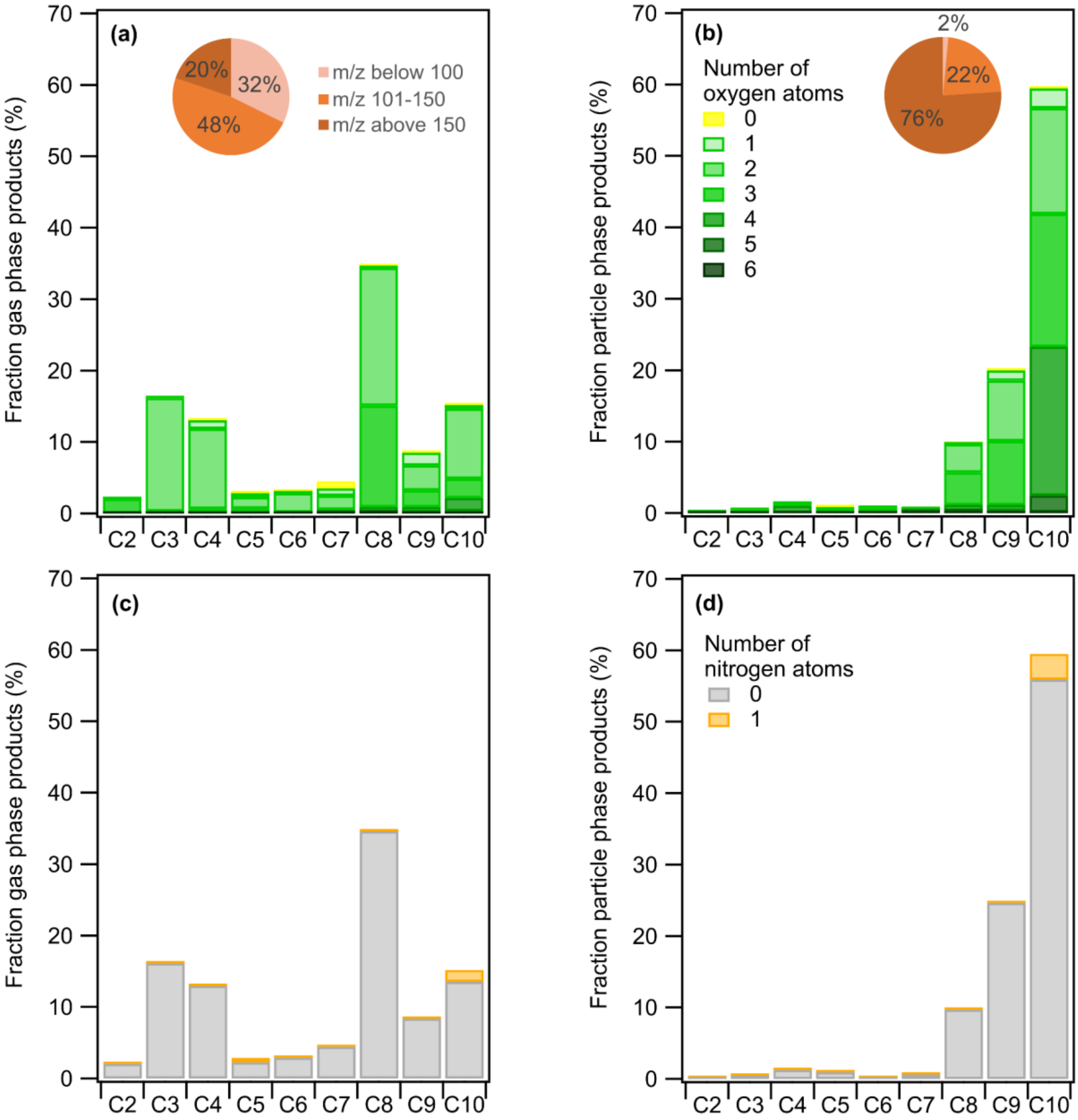

Figure S4. Naphthalene mass products fraction (y-axis) distribution based on the number of carbon atoms (x-axis) for a high NO_x experiment 295 K, colored by the number of (a,b) oxygen and (c,d) nitrogen atoms. Detected compounds are in the (a,c) gas phase and (b,d) particle phase. Pie charts correspond to the molecular weight contribution to the overall mass.

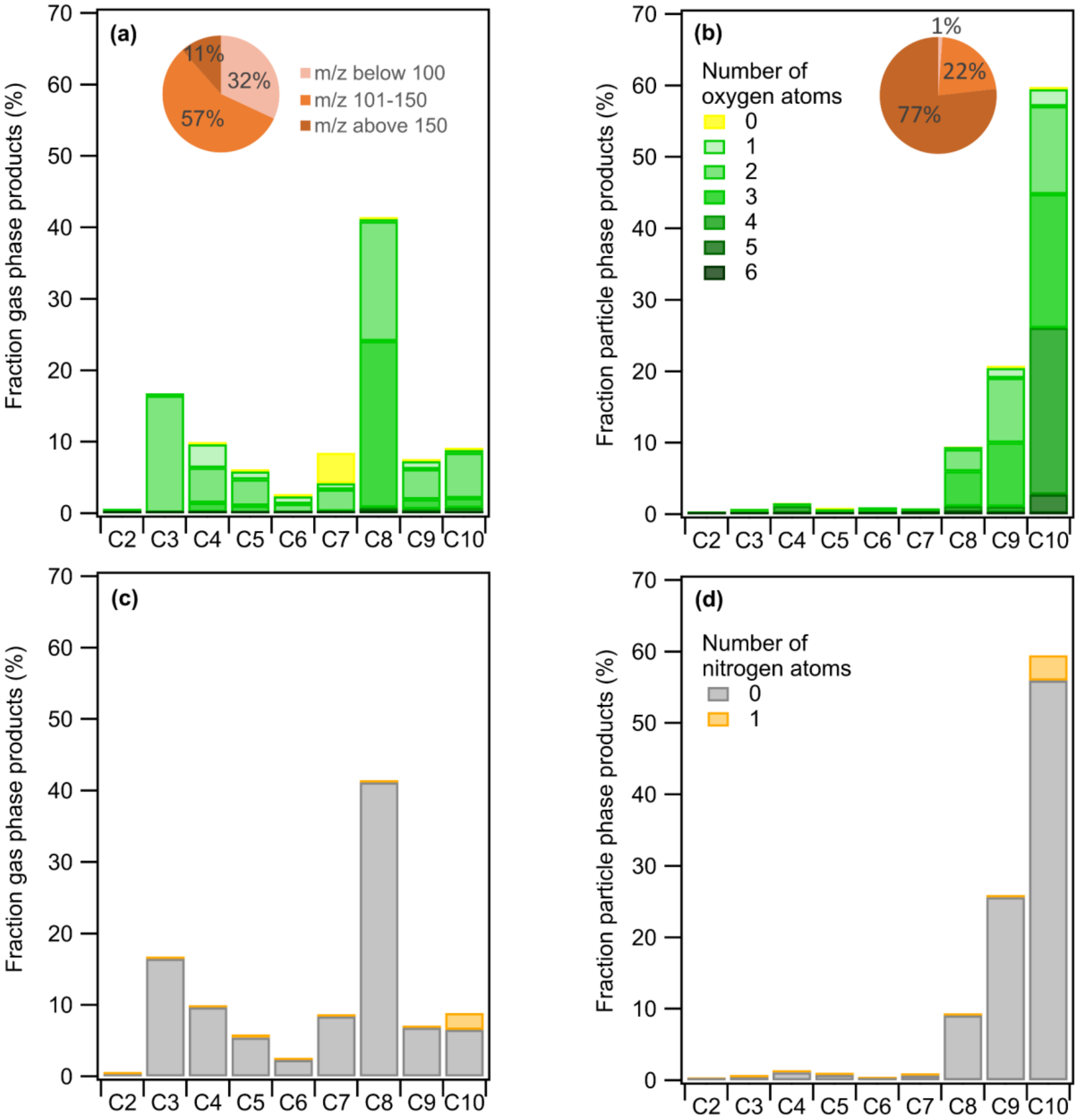

Figure S5. Naphthalene mass products fraction (y-axis) distribution based on the number of carbon atoms (x-axis) for a low NO_x experiment 295 K, colored by the number of (a,b) oxygen and (c,d) nitrogen atoms. Detected compounds are in the (a,c) gas phase and (b,d) particle phase. Pie charts correspond to the molecular weight contribution to the overall mass.

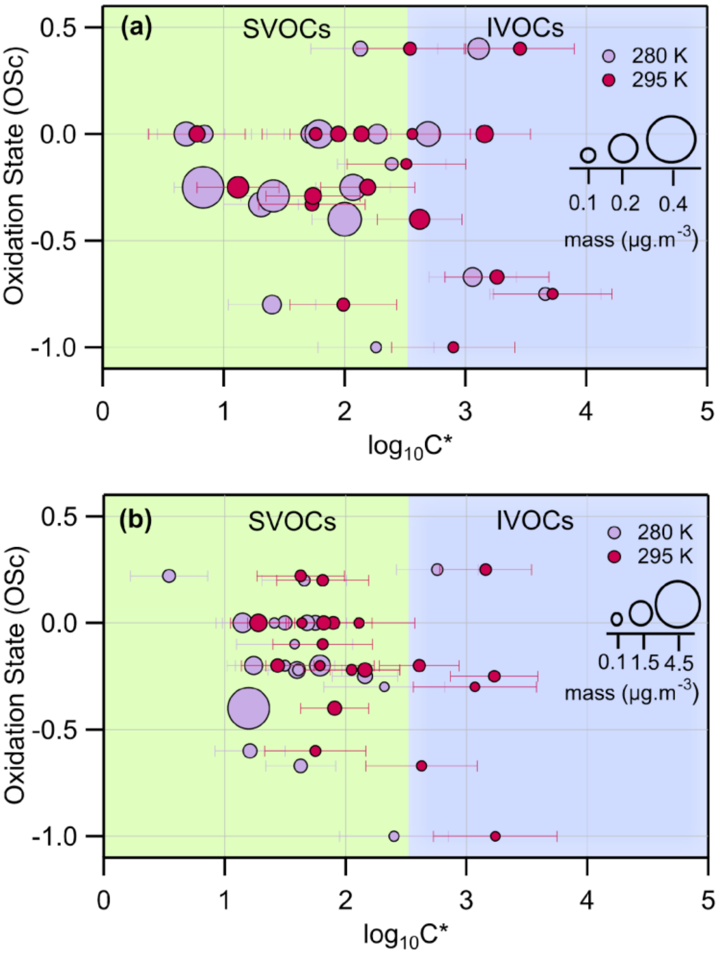

Figure S6. **The OSc (y-axis) for the detected parent ions of (a) m-xylene and (b) naphthalene photooxidation, respectively, as a function of saturation concentration ($\log_{10}C_i^*$ in µg m^{-3}; x-axis) for high NO$_x$ experiments. The size of the circles denotes the mass of each species. Experiments carried out at 280 K are in light violet while the ones carried out at 295 K are in magenta.**

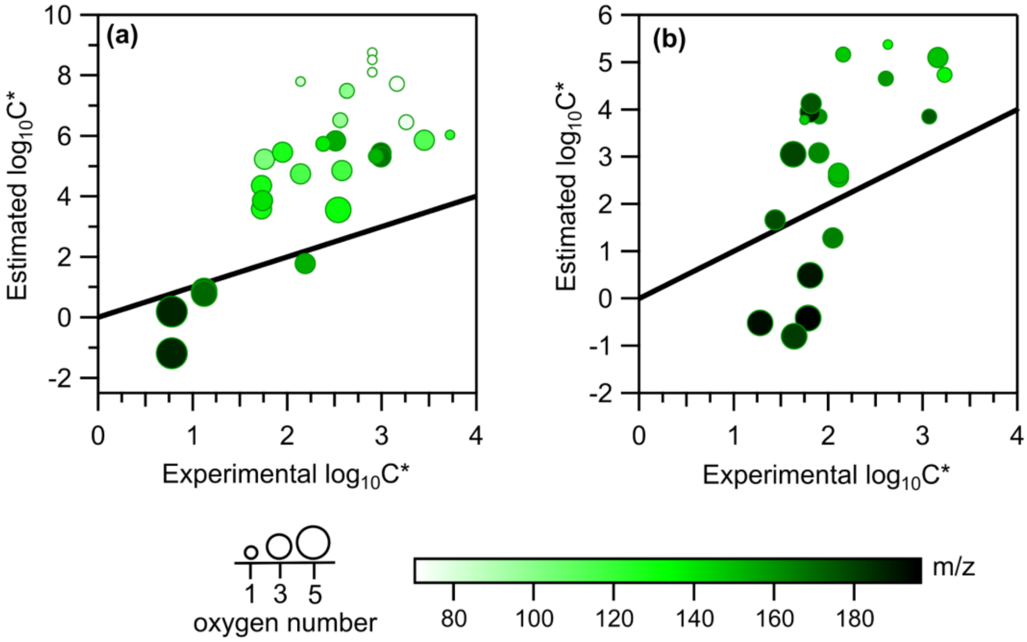

Figure S7. Theoretical (y-axis) versus experimental log$_{10}$*C_i^** values (x-axis) for (a) m-xylene and (b) naphthalene oxidation products at 295 K under high NO$_x$ conditions. The black line is the 1:1 fit. The size of the markers is proportional to the oxygen number. The color gradient corresponds to *m*/*z* of the detected compounds.

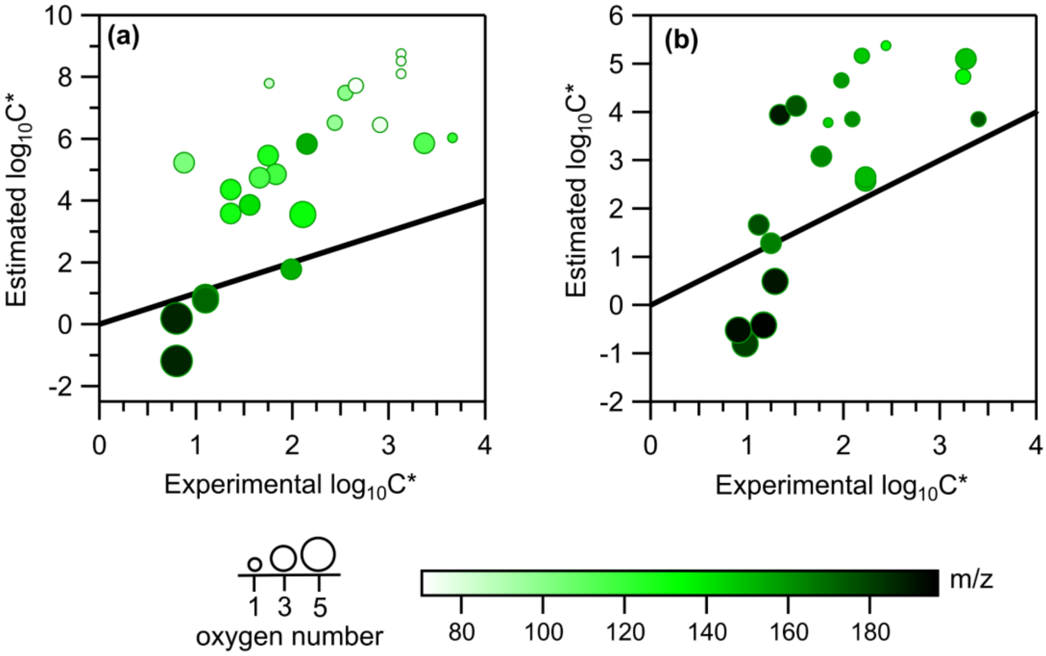

Figure S8. Theoretical (y-axis) versus experimental log$_{10}$*C_i^** values (x-axis) for (a) m-xylene and (b) naphthalene oxidation products at 295 K under low NO$_x$ conditions. The black line is the 1:1 fit. The size of the markers is proportional to the oxygen number. The color gradient corresponds to *m*/*z* of the detected compounds.

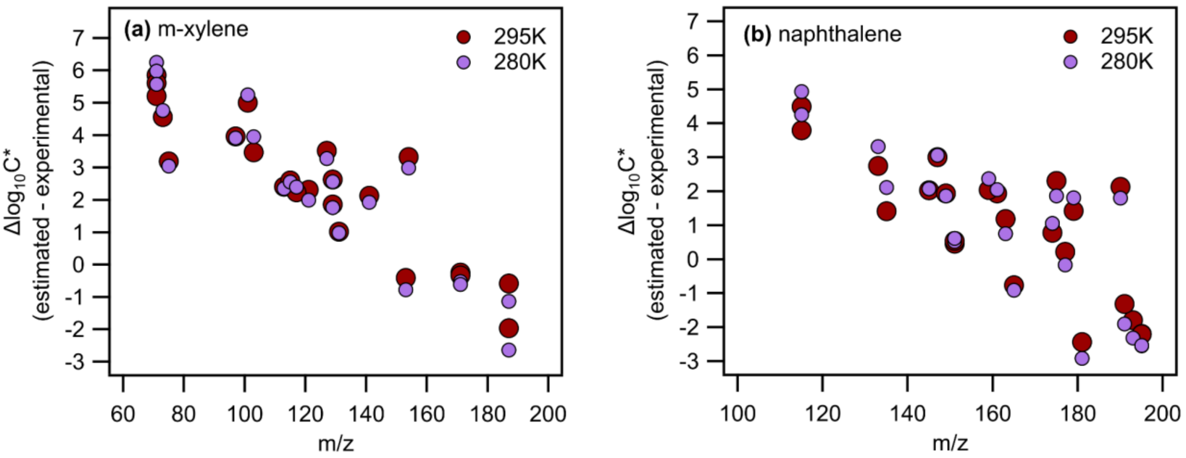

Figure S9. $\Delta\log_{10}C_i^*$ ($\log_{10}C_i^*$ Estimated minus $\log_{10}C_i^*$ Experimental; y-axis) versus *m*/*z* (x-axis) for (a) m-xylene and (b) naphthalene oxidation products under high NO_x conditions, at 295 K (magenta) and 280 K (light violet).